Optical Engineering

SPIEDigitalLibrary.org/oe

1×4 signal router using three Mach-Zehnder interferometers

Sanjeev Kumar Raghuwanshi
Ajay Kumar
Santosh Kumar

1 × 4 signal router using three Mach-Zehnder interferometers

Sanjeev Kumar Raghuwanshi
Ajay Kumar
Santosh Kumar
Indian School of Mines
Department of Electronics Engineering
Photonics Lab
Dhanbad 826004, India
E-mail: santoshrus@ismu.ac.in

Abstract. This paper presents an overview of integrated optical signal routing based on the principle of electro-optic effects. There are some specific types of materials whose refractive index changes due to the application of the electric field. Lithium-niobate ($LiNbO_3$) and gallium arsenide are some important electro-optic materials. Due to the application of the voltage across electrode present in one of the arms of Mach-Zehnder interferometer (MZI), the electric field changes, hence, phase change in the signal present in one of the arms. Depending upon the phase change introduced, signal shifts from one waveguide to the other waveguide. Hence, this paper provides the detailed description of 1 × 4 signal router, using three MZI, and its construction using beam propagation method. Finally, the results are verified by the MATLAB-based results. [DOI: 10.1117/1.OE.52.3.035002]

Subject terms: signal router; Mach-Zehnder interometer; linear waveguide; S-bend sine waveguide; beam propagation method.

Paper 121804 received Dec. 8, 2012; revised manuscript received Jan. 28, 2013; accepted for publication Feb. 4, 2013; published online Mar. 4, 2013.

1 Introduction

Curvilinear directional couplers, branching and combining waveguides, S-shaped bend waveguides, and tapered waveguides are indispensable components in constructing an integrated optical circuit. In practical directional couplers, however, light coupling in the S-shaped bend waveguide regions, in the front and rear of parallel waveguides, should be taken into account in order to evaluate the propagation characteristics precisely. Optical interferometer circuits, composed of optical couplers and optical delay parts, are a basic element employed in various optical devices.[1–3] Such circuits include Mach-Zehnder interferometers (MZIs), lattice-form filters (or cascaded MZIs), transversal-form filters, and interferometers with ring resonator filters.[4–8] Treyz[9] showed the silicon Mach-Zehnder waveguide interferometers operating at wavelength 1.3 μm. This presented the switching mechanism based on the thermally induced variation of the refractive index of crystalline silicon. Besse et. al. explained about the optical switches based on Mach-Zehnder configuration with improved extinction ratios.[10] They study driving conditions to improve the extinction ratios in 2 × 2 and 1 × 2 all-optical switches based on semiconductor optical amplifiers in Mach-Zehnder configuration. Hu et al. used symmetric and asymmetric Y-branches, employing height-tapered waveguides, in order to achieve power splitting and mode sorting, respectively, in the interferometer.[11] Yoshimoto et al. proposed the polarization-insensitive MZI switch that is useful for optical gate elements.[12] This is especially well suited to wavelength-division multiplexing network components. Lagali et. al. proposed the generalized MZIs for variable ratio power splitting and optimized switching.[13] They analyzed the nonideal integrated optical $N \times N$ generalized MZI (GMZI) employing multimode interference (MMI) couplers using the transfer matrix technique. Schreieck et al. presents the results of cross-gain and cross-phase modulation experiments on InGaAsP-based semiconductor optical amplifiers and MZI switches.[14] Tol et al. presents an MZI-based low-loss combiner.[15] They have shown a nonlinear MZI to provide the combiner function without control signals and nonlinear effect caused by carrier depletion in the semiconductor optical amplifiers (SOAs). Zheng et al. introduced the three-dimensional (3-D) mode propagation analysis and point matching method which presents a novel formulation technique to analyze the low- and high-frequency characteristics for the impedance-matched polymer MZI electro-optic (EO) switch based on MMI couplers.[16] Mizuno et al. presented a theoretical and experimental study of an optical interferometer circuit with a uniform wavelength spacing.[17] Kumar et al. proposed a simple all-optical logic device, called MZI, which is composed by using an SOA and an optical coupler.[18] Raghuwanshi et al.[19] studied the Y-branch having inbuilt optical splitters and combiner using beam propagation method (BPM).[19]

This paper outlines the design process of a signal router based on integrated three MZIs. An EO switch is a device used in integrated fiber optics. The device is based on MZI and is made by titanium diffusion in lithium niobate substrate. The switching between the ports is achieved by an EO effect within the structure. Voltage, applied to the electrodes deposited on the integrated MZI, creates an electric field distribution within the substrate which, consequently, changes its refractive index. If properly designed, the induced change, in the refractive index, leads to different coupling between individual ports. In Sec. 2, we explain about the EO effect. Section 3 explains about the formation of signal router and Sec. 4 presents and discusses the results obtained from BPM and MATLAB.

2 Electro-Optic Effect

Switches and couplers fall in the categories of integrated optical devices. In fact, as the name suggests, the devices, which can be fabricated on a wafer, are known as integrated

optical devices. Essentially, we are creating the light guiding environment on the substrate so the circuit, essentially, looks like an integrated circuit. That is why it is given the name integrated device. In this paper, we are creating a waveguide structure on a substrate and sending the signal from optical fiber to these devices. The property of light is changed, then the light is launched back again into an optical fiber. At the heart of the integrated optical devices, a phenomenon called the EO effect occurs. Refractive index of the material changes with application of electric field. Lithium-niobate (high degree of loss but high EO coefficient) and gallium arsenide (low EO coefficient) are some important EO materials. The change in the refractive index is given by the L28-Integrated Optics-I. video in Ref. 20.

$$\Delta n = \left(\frac{n^3}{2}\right) rE, \tag{1}$$

where r is EO coefficient and E is the electric field. We have certain materials whose dielectric constant can be changed by the application of an electric field or magnetic field. If we consider a material that changes the dielectric constant due to an application of electromagnetic field across it, then those types of material are called EO material. If the dielectric constant changes due to the application of magnetic field, then those types of material are known as magneto-optic materials. Here, we want to make use of EO material and the effect that the dielectric material changes by the application of electric field is called EO effect. Gallium arsenide required high electric field to realize the same changes as in lithium niobate; however, there is less loss when this material is used.

Basically, lithium niobate is an anisotropic material; therefore, the refractive index and dielectric constant remain different in different directions when the electric field is applied. In short, we can say that, we have the material in which the refractive index can change with the application of electric field. This effect is also known as the Pockel effect. The Pockel effect states that the refractive index changes proportional to the applied electric field. Now, by using the property of the material, we essentially can alter the characteristics of the light passing through the material and we can write the phase changes due to the applied electric field as[20]

$$\Delta\varphi = \frac{2\pi}{\lambda}(\Delta n)L. \tag{2}$$

Now, from Eq. (1), we can write

$$\Delta\varphi = \frac{2\pi}{\lambda}\left[\left(\frac{n^3}{2}\right) rE\right]L. \tag{3}$$

For a given device, and for an optical signal, λ is constant and n is a constant refractive index of the substrate material. The EO coefficient of the material is constant. Therefore, essentially, we have the product of E and L. If we use the high value of the electric field, the length required remains reasonably small, but the change in the refractive index is very small. The change in the refractive index is typically 2×10^{-6}. So to get a substantial phase change into the light, we require a significant length for the propagation of light. Hence, it is immediately clear that since Δn is very small, we require a length, typically of the order of a few millimeters, to obtain the substantial phase change in the light output. When the gap between the electrodes is reduced, electric field is increased and the size of the device is reduced to a few millimeters in length in order to get the substantial change in the phase of the device. These parameters are shown in Table 1. Let us say, if the voltage difference between these two electrodes is V and d is the separation between the electrodes, then electric field will be approximately V/d. Hence, we can write

Table 1 Different parameters to obtain particular voltage V_π.

Parameters	Value of parameters
Wavelength (λ)	1.33 μm
Separation between the electrode (d)	6 μm
Refractive index	1.47
Electro-optic coefficient	3.66×10^{-10} m/V
Substantial length (L)	10,000 μm

$$\Delta\varphi = \frac{2\pi}{\lambda}\left[\left(\frac{n^3}{2}\right)\frac{V}{d}r\right]L. \tag{4}$$

Therefore, when no voltage is applied, $\Delta\varphi$ remains zero, and when we apply the voltage (V) the phase is changed by π. This particular voltage is known as V_π. Hence, we can write

$$V_\pi = \frac{\lambda}{n^3}\frac{1}{r}\frac{d}{L}. \tag{5}$$

To get the corresponding value of V, we require substantial length L. d cannot be reduced significantly. If we try to reduce d, then electric field will be partly inside and outside; consequently, field strength might be larger than the breakdown field. Separation cannot be less than a few microns. Essentially, d cannot be decreased to get the value V_π. Therefore, there is limitation on all these quantities. Thus, for substantial length V_π, voltage remains very low. So, this is basic for a module which works on the principle of EO effect and the phase of the signal which can be changed by the application of the signal voltage across the channel waveguide as the frequency of the signal increases. Due to the application of the electric field, the phase difference changes and, hence, coupling length of the device changes due to which signal shifts in the other waveguide.

3 Formation of the Signal Router

The idea of MZI is very simple. Here, we show the plan on lithium niobate. We have a substrate, which is lithium niobate, and above the substrate, we have created the channel waveguide as shown in Fig. 1. The device contains two input ports and two output signal ports associated with electrode, so that can change the refractive index of one of the arms. Light is brought and we have two-way power divider so that the light gets equally divided into two parts, propagates in the arms, and again combines. It requires equal combiner

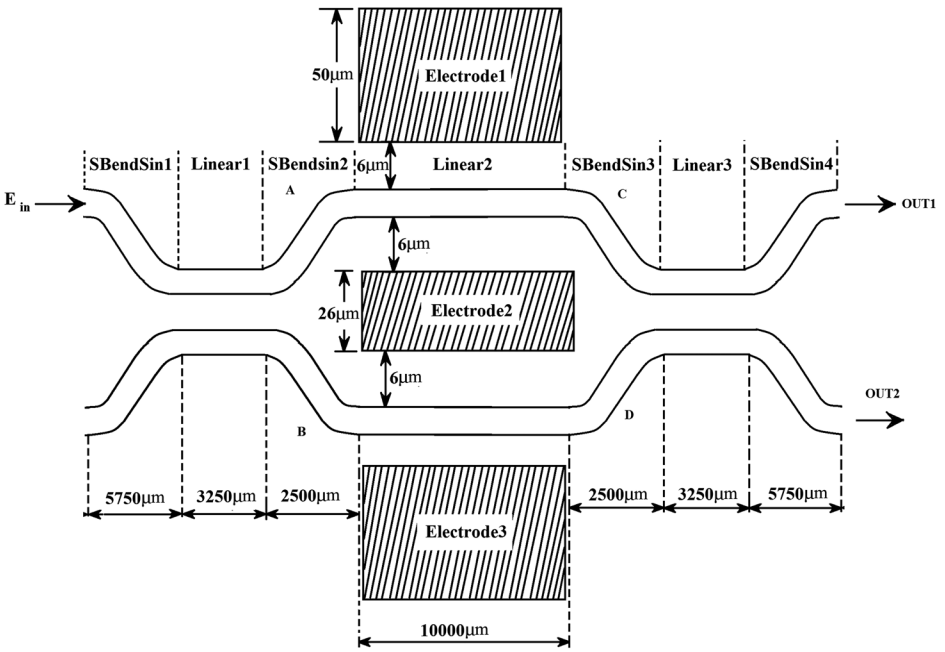

Fig. 1 Basic schematic view of Mach-Zehnder interferometer with proper electrode.

and finally signal gets combined and splits into two ports using a signal splitter.[19] Assuming that the two have exactly identical paths, the signal reaches in phase, so whatever signal is given in input, the same signal can be obtained at the output. Let us now say that we put an electrode around this. Therefore, we have created a phase modulator around one of the arms of this MZI. Now, we can apply the voltage across the electrode.

So, when zero voltage is applied to one of the arms, in this case, constructive interference takes place. When the voltage is applied, destructive interference takes place. Now, the signal is allowed to pass through the 3-dB coupler. So, on the basis of phase difference introduced on the two arms the signals are divided on the two output ports; we can apply the same concept in order to obtain the signal router or de-multiplexers. We can write the equation as follows:

$$A = \sqrt{1-\alpha_1}(E_{\text{in}}) + j\sqrt{\alpha_1}(0), \tag{6}$$

$$B = j\sqrt{\alpha_1}(E_{\text{in}}) + \sqrt{1-\alpha_1}(0), \tag{7}$$

where α_1 is attenuation constant of first directional coupler represented toward the input side of Fig. 1. In matrix form, it can be represented as follows:

$$\begin{bmatrix} A \\ B \end{bmatrix} = \begin{bmatrix} \sqrt{1-\alpha_1} & j\sqrt{\alpha_1} \\ j\sqrt{\alpha_1} & \sqrt{1-\alpha_1} \end{bmatrix} \begin{bmatrix} E_{\text{in}} \\ 0 \end{bmatrix}. \tag{8}$$

Similarly, we can write

$$C = Ae^{-j\varphi_1} \tag{9}$$

$$D = Be^{-j\varphi_2}. \tag{10}$$

In matrix form, we can write

$$\begin{bmatrix} C \\ D \end{bmatrix} = \begin{bmatrix} e^{-j\varphi_1} & 0 \\ 0 & e^{-j\varphi_2} \end{bmatrix} \begin{bmatrix} A \\ B \end{bmatrix}. \tag{11}$$

In the case of second coupler, we can write the equation as follows:

$$\text{OUT}_1 = \sqrt{1-\alpha_2}(C) + j\sqrt{\alpha_2}(D) \tag{12}$$

$$\text{OUT}_2 = j\sqrt{\alpha_2}(C) + \sqrt{1-\alpha_2}(D). \tag{13}$$

In Eqs. (10) and (11), α_2 represents the attenuation constant of the second directional coupler, represented toward the output side of Fig. 1. We can represent Eqs. (10) and (11) in matrix form as follows:

$$\begin{bmatrix} \text{OUT}_1 \\ \text{OUT}_2 \end{bmatrix} = \begin{bmatrix} \sqrt{1-\alpha_2} & j\sqrt{\alpha_2} \\ j\sqrt{\alpha_2} & \sqrt{1-\alpha_2} \end{bmatrix} \begin{bmatrix} C \\ D \end{bmatrix}. \tag{14}$$

Now putting the values of C, D, A, and B from Eqs. (8) and (11) in Eq. (14), we get

$$\text{OUT}_1 = [\sqrt{1-\alpha_1}\sqrt{1-\alpha_2}e^{-j\varphi_1} - \sqrt{\alpha_1}\sqrt{\alpha_2}e^{-j\varphi_2}]E_{\text{in}} \tag{15}$$

$$\text{OUT}_2 = j[\sqrt{\alpha_1}\sqrt{1-\alpha_2}e^{-j\varphi_1} + \sqrt{\alpha_2}\sqrt{1-\alpha_1}e^{-j\varphi_2}]E_{\text{in}}. \tag{16}$$

In order to achieve the highest extinction ratio $\alpha_1 = \alpha_2 = 0.5$. In this case, the extinction ratio can be represented as the ratio of the maximum and the minimum power levels of the transfer function. Hence, if the minimum power level of the transfer function is zero, we have the infinite extinction ratio. Basically, to achieve the highest extinction ratio, we require 50% of the power splitting ratio for optical couplers. Hence, ideally, the couplers used in

designing the device must have the attenuation constants 0.5. Hence, we can write

$$\mathrm{OUT}_1 = \frac{1}{2}[e^{-j\varphi_1} - e^{-j\varphi_2}]E_{\mathrm{in}}.$$

After simplification, we can write

$$\mathrm{OUT}_1 = je^{-j(\varphi_0)} \sin\left(\frac{\Delta\varphi}{2}\right)E_{\mathrm{in}}. \quad (17)$$

In the same manner, we can write

$$\mathrm{OUT}_2 = j\frac{1}{2}[e^{-j\varphi_1} + e^{-j\varphi_2}]$$

$$\mathrm{OUT}_2 = je^{-j(\varphi_0)} \cos\left(\frac{\Delta\varphi}{2}\right)E_{\mathrm{in}}, \quad (18)$$

where we assume that $\frac{\varphi_1+\varphi_2}{2} = \varphi_0$, and $\varphi_1 - \varphi_2 = \Delta_\varphi$.

Now, normalized power at port 1 and port 2 can be represented as follows:

$$P_{\mathrm{out1}} = \left|\frac{\mathrm{OUT}_1}{E_{\mathrm{in}}}\right|^2 = \left|je^{-j(\varphi_0)} \sin\left(\frac{\Delta\varphi}{2}\right)\right|^2 = \sin^2\left(\frac{\Delta\varphi}{2}\right) \quad (19)$$

$$P_{\mathrm{out2}} = \left|\frac{\mathrm{OUT}_2}{E_{\mathrm{in}}}\right| = \left|je^{-j(\varphi_0)} \cos\left(\frac{\Delta\varphi}{2}\right)\right|^2 = \cos^2\left(\frac{\Delta\varphi}{2}\right). \quad (20)$$

Here, φ_1 and φ_2 are the phase differences that arise due to application of the voltage across the electrode, where $\varphi_1 = \frac{\pi}{V_\pi}V_1$ and $\varphi_2 = \frac{\pi}{V_\pi}V_2$.

Hence, depending upon the phase difference, signal shifts from one port to another port. By using this configuration, we can make the signal router. The block diagram of the signal router is given in Fig. 2. This block diagram is a combination of the three MZIs. Each MZI is capable of switching the signal on the second waveguide depending upon the voltage given at the electrode.

Figure 3 shows the combination of three MZIs. The two outputs, obtained from the first MZI, are connected to the input of the second and third MZI. Now, by applying the voltage at electrode 2 of each MZI, we can either keep the signal in the same arm or shift the signal into the other

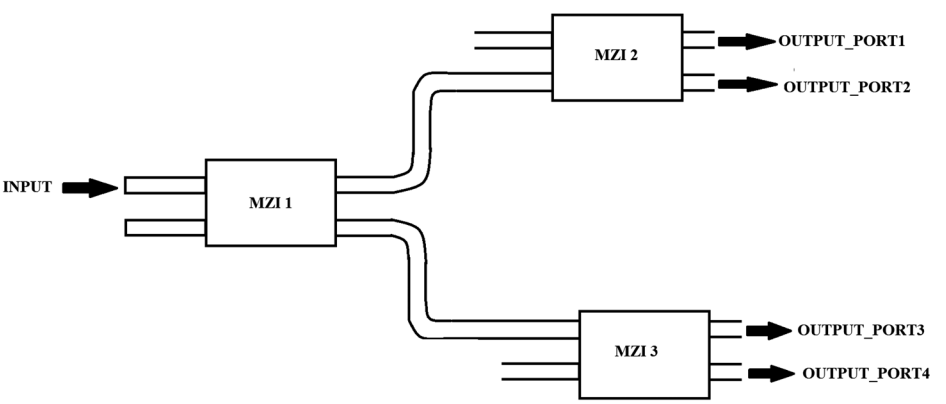

Fig. 2 Block diagram of a signal router using three Mach-Zehnder interferometers.

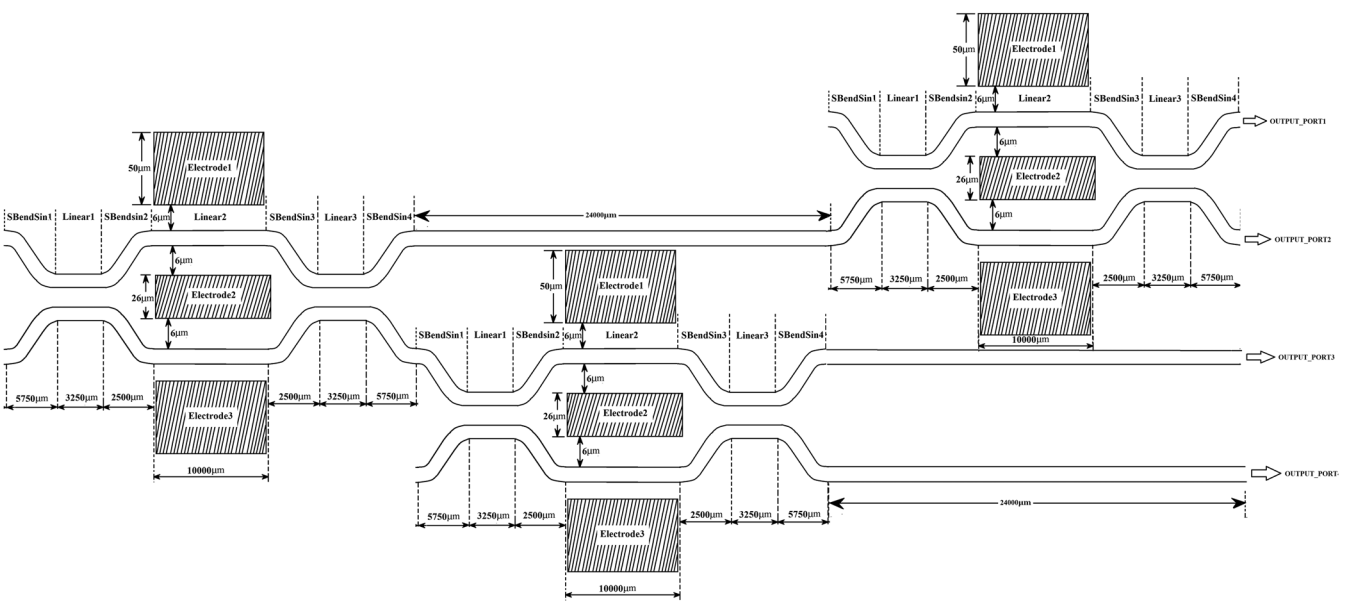

Fig. 3 Signal router using three Mach-Zehnder interferometers.

arm depending upon the applied voltage. In this process, we have grounded electrode 1 and electrode 3.

Basically, due to application of proper voltage ($V_2 = 6.75$ V) for the applied parameter and path length, the signal remains in the same waveguide. Various parameters are shown in Table 1 to obtain particular voltage (V_π), hence we obtained the value of V_π as 6.75 V. Similarly, when no potential difference is applied across electrode 2, signal shifts into the second waveguide. These explanations can be proven using Eqs. (19) and (20). Hence, by applying the appropriate control signal, which is nothing but the potential applied at electrode 2 of each MZI, we can select any output port among the four output ports. Therefore, the system can be used as a signal router. Here, crystal material is lithium niobate and its propagation direction is in Y direction. The waveguides of MZI are created by the diffusion of titanium in lithium niobate substrate. Width of waveguide is 8 microns and material used for waveguide is $TiLiNbO_3$.

We have specified an electrode region with three electrodes, all with zero voltage, positioned slightly off the symmetry axis of the MZI. Table 2 shows the different simulation parameters. Now, the same structure is created twice in order to obtain the structure of signal router.

Table 2 Simulation parameters.

Reference index	Modal
Wavelength	1.3 μm
Polarization	Transverse magnetic
Mesh-number of points	500
BPM solver	Paraxial
Engine	Finite difference
Scheme parameter	0.5
Propagation step	1.3
Boundary condition	Transparent boundary condition (TBC)

4 Results and Discussion

Finally, we used the BPM by applying the various combinations of the control signal (the voltage at the electrode of each MZI, keeping other two electrodes grounded of each MZI). Now, with the application of the various control signals, the outputs are shown in Fig. 4.

Figure 4 shows the travelling of the input signal up to various ports depending upon the choice of the control signal s_1, s_2, and s_3. Figure 4(a) shows that input signal approaches toward output port 1 as we have applied control signal $s_1 = 6.75$ V, $s_2 =$ 'X' (can be 6.75 V or 0 V), and $s_3 = 0$ V. We can see that, due to application of the control signal $s_1 = 6.75$ V, the signal exists in the same waveguide as the phase difference is π. However, due to application of the control signal $s_3 = 0$, shift of the signal from one arm to the second arm takes place, and, finally, whole signal appears on output port 1. Similarly, we can select the output port 2 by making the choice $s_1 = 6.75$ V, $s_2 =$ 'X', and $s_3 = 6.75$ V as shown in Fig. 4(b). Hence, by making the choice $s_3 = 6.75$ V, we can introduce the phase shift of π in the third MZI. Therefore, the signal exists in the same arm of the third MZI and output port 2 can be selected. By applying the same concept, we can obtain the output at output port 3 and output port 4, respectively. We can represent the combination of the control signals s_1, s_2, and s_3 for obtaining the output at the various ports in Table 3, where "X" is considered as "don't care" (either 6.75 V or 0 V).

We can generate the above result, using MATLAB, by applying the proper mathematical expression. From Fig. 4,

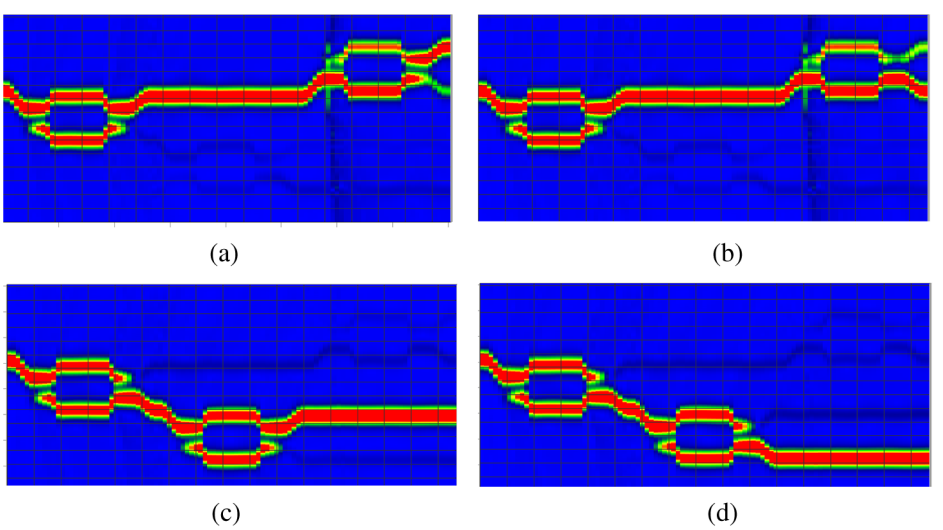

Fig. 4 The optical field propagation at various output ports depending upon the control signal s_1, s_2, and s_3, where s_1, s_2, and s_3 are the voltage applied at the second electrode of first, second, and third MZI. (a) Output signal at port 1 for control signal $s_1 = 6.75$ V, $s_2 =$ 'X' (can be 6.75 V or 0 V), and $s_3 = 0$ V. (b) Output signal at port 2 for the control signal $s_1 = 6.75$ V, $s_2 =$ 'X', and $s_3 = 6.75$ V. (c) Output signal at port 3 for the control signal $s_1 = 0$ V, $s_2 = 6.75$ V, and $s_3 =$ 'X'. (d) Output signal at port 4 for the control signal $s_1 = 0$ V, $s_2 = 0$ V, and $s_3 =$ 'X', where X is treated as don't care conditions.

Table 3 The output power at the four output ports on the basis of control signal s_1, s_2, and s_3.

s_1	s_2	s_3	Output_ port1	Output_ port2	Output_ port3	Output_ port4
6.75 V	"X"	0 V	1	0	0	0
6.75 V	"X"	6.75 V	0	1	0	0
0 V	6.75 V	"X"	0	0	1	0
0 V	0 V	"X"	0	0	0	1

Table 4 Various parameters for $\Delta\phi_1$, $\Delta\phi_2$, $\Delta\phi_3$.

Parameters	Parameters for getting the output signal at PORT 1	Parameters for getting the output signal at PORT 2	Parameters for getting the output signal at PORT 3	Parameters for getting the output signal at PORT 4
V_1	6.75 V	6.75 V	0 V	0 V
V_2	0 V	0 V	6.75 V	0 V
V_3	0 V	6.75 V	0 V	6.75 V
$\Delta\phi_1$	$\frac{\pi}{V\pi}(V_1 - V_2)$	$\frac{\pi}{V\pi}(V_1 - V_2)$	$\frac{\pi}{V\pi}(V_1 - V_3)$	$\frac{\pi}{V\pi}(V_1 - V_2)$
$\Delta\phi_2$	$\frac{\pi}{V\pi}(V_2)$	$\frac{\pi}{V\pi}(V_2)$	$\frac{\pi}{V\pi}(V_2 - V_3)$	$\frac{\pi}{V\pi}(V_2)$
$\Delta\phi_3$	$\frac{\pi}{V\pi}(V_3 - V_2)$	$\frac{\pi}{V\pi}(V_3 - V_2)$	$\frac{\pi}{V\pi}(V_3)$	$\frac{\pi}{V\pi}(V_3 - V_2)$

we can write the mathematical expression for the normalized output power at the ports 1, 2, 3, and 4 as follows:

$$P_{\text{out1}} = \cos^2\left(\frac{\Delta\varphi_3}{2}\right)\sin^2\left(\frac{\Delta\varphi_1}{2}\right), \quad \text{when } s_1 = 6.75 \text{ V}, \quad s_2 = X, \quad \text{and} \quad s_3 = 0 \text{ V} \tag{21}$$

$$P_{\text{out2}} = \sin^2\left(\frac{\Delta\varphi_3}{2}\right)\sin^2\left(\frac{\Delta\varphi_1}{2}\right), \quad \text{when } s_1 = 6.75 \text{ V}, \quad s_2 = X, \quad \text{and} \quad s_3 = 6.75 \text{ V} \tag{22}$$

$$P_{\text{out3}} = \sin^2\left(\frac{\Delta\varphi_2}{2}\right)\cos^2\left(\frac{\Delta\varphi_1}{2}\right), \quad \text{when } s_1 = 0 \text{ V}, \quad s_2 = 6.75 \text{ V}, \quad \text{and} \quad s_3 = X \tag{23}$$

$$P_{\text{out4}} = \sin^2\left(\frac{\Delta\varphi_2}{2}\right)\sin^2\left(\frac{\Delta\varphi_1}{2}\right), \quad \text{when } s_1 = 0 \text{ V}, \quad s_2 = 0 \text{ V}, \quad \text{and} \quad s_3 = X. \tag{24}$$

Table 4 shows the various parameters for $\Delta\phi_1$, $\Delta\phi_2$, $\Delta\phi_3$. Figures 5 to 8 show the MATLAB plots of the normalized output power at ports 1, 2, 3, and 4. Figure 5 shows the stepwise variation in normalized output power, at ports 1, 2, 3, and 4, due to the application of the control signal $s_1 = 6.75$ V, $s_2 =$ 'X', and $s_3 = 0$ V. Finally, the output exists at port 1 only on the voltage $s_1 = 6.75$ V. Similarly, Fig. 6 shows the stepwise variation in normalized output power, at ports 1, 2, 3, and 4, due to the application of the control signal $s_1 = 6.75$ V, $s_2 =$ 'X', and $s_3 = 6.75$ V. Figure 7 shows the output power at port 3 exists on the

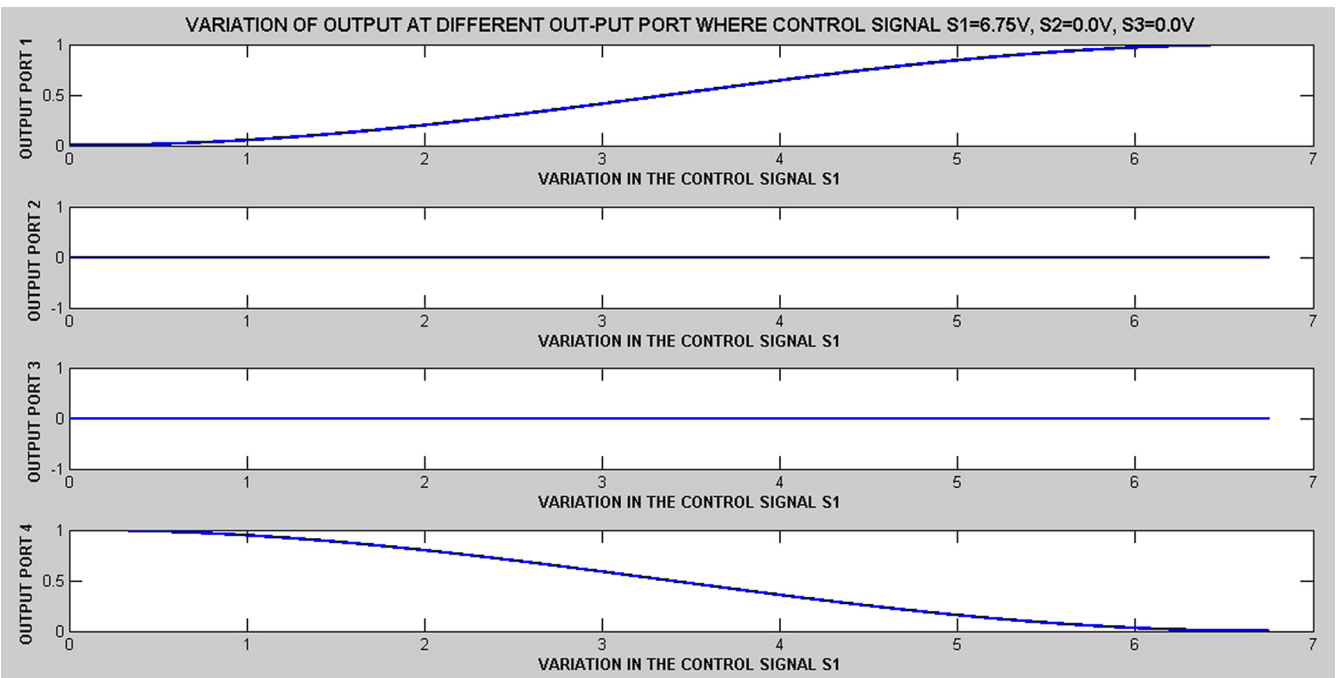

Fig. 5 The variation of the output power at ports 1, 2, 3, and 4 due to the variation in control signal s_1 (applied control signals are $s_1 = 6.75$ V, $s_2 =$ 'X', and $s_3 = 0$ V).

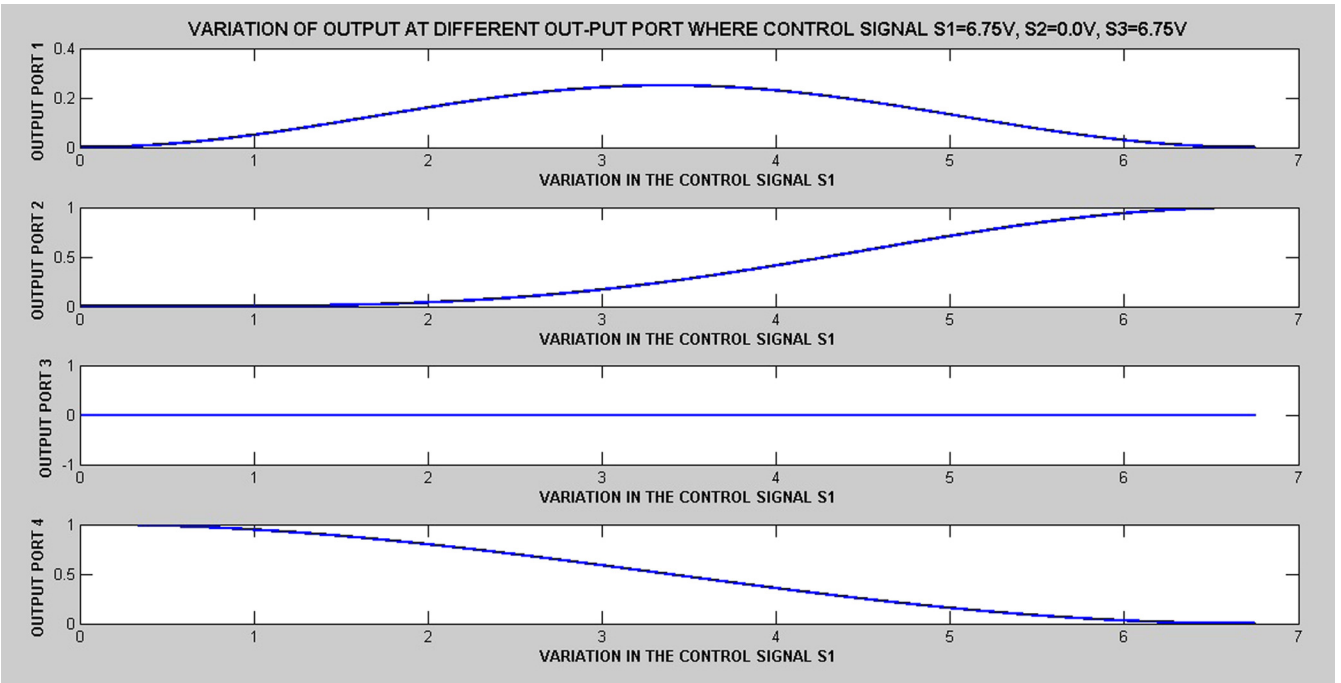

Fig. 6 The variation of the output power at ports 1, 2, 3, and 4 due to the variation in control signal (applied control signals are $s_1 = 6.75$ V, $s_2 =$ 'X', and $s_3 = 6.75$ V.

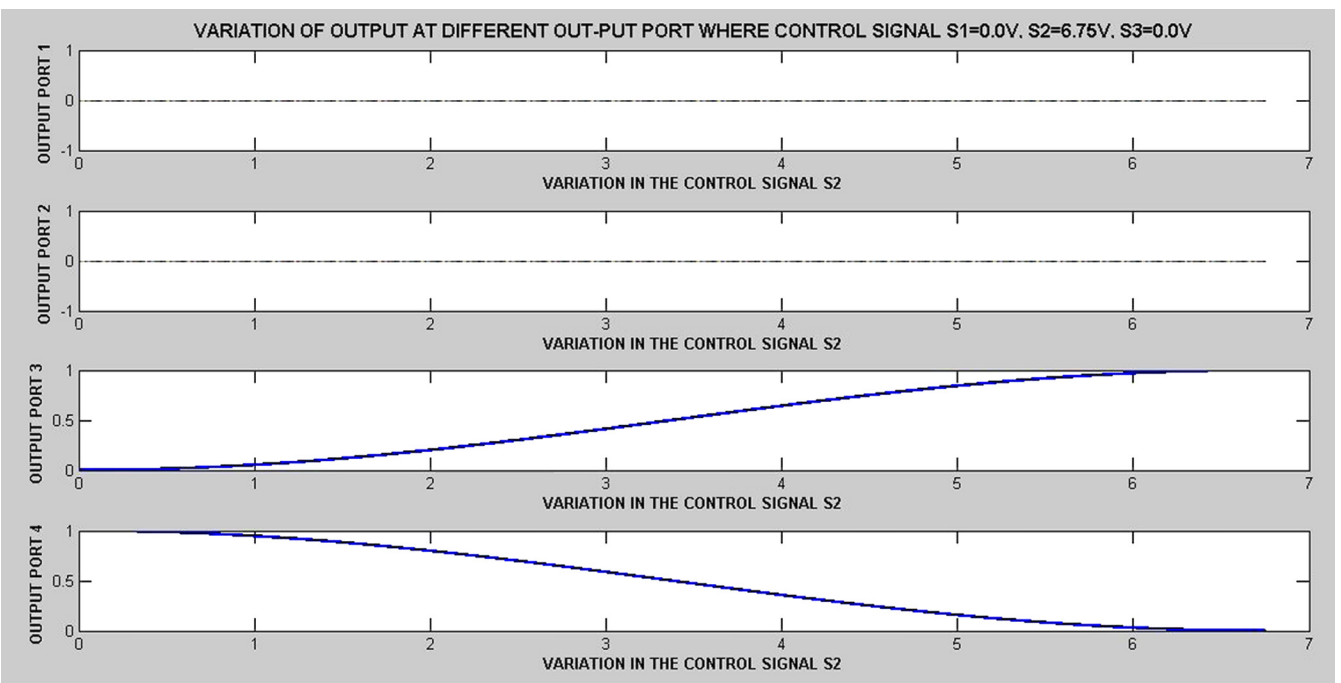

Fig. 7 The variation of the output power at ports 1, 2, 3, and 4 due to the variation in control signal s_2 (applied control signals are $s_1 = 0$ V, $s_2 = 6.75$ V, and $s_3 =$ 'X').

voltage signal $s_1 = 0$ V, $s_2 = 6.75$ V, and $s_3 =$ 'X'. In the same manner, Fig. 8 shows the result of the output power at port 4.

5 Conclusion

We have designed the 1 × 4 signal router by the combination of the three MZIs. The switching between the ports can be achieved by an EO effect within such type of structure. Voltage, applied to the electrodes deposited on the integrated MZI, creates an electric field distribution within the substrate which, consequently, changes its refractive index. Due to variation of the refractive index, phase difference arises; hence, depending upon the phase, signals shift from one waveguide to another waveguide. Using this concept, we have implemented the signal router and run the BPM simulation to find out the optimum values of the electrode

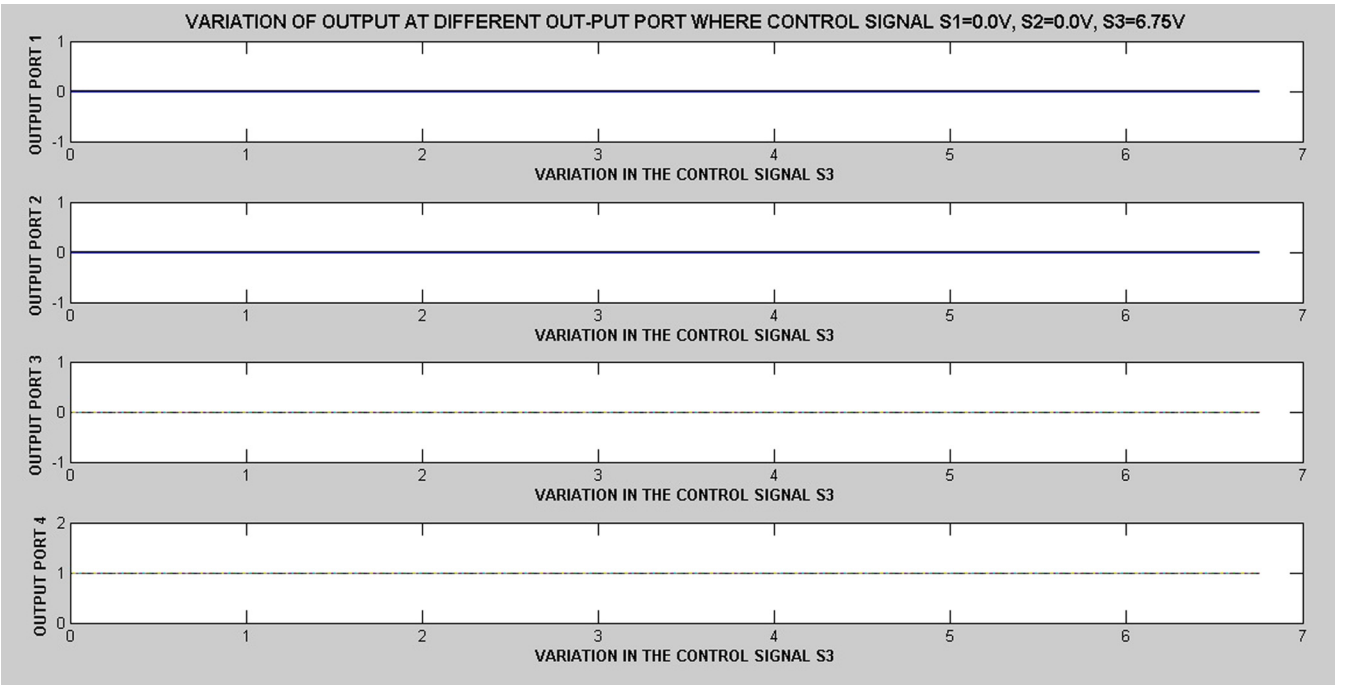

Fig. 8 The variation of the output power at ports 1, 2, 3, and 4 due to the variation in control signal s_3 (applied control signals are $s_1 = 0$ V, $s_2 = 0$ V and $s_3 =$ 'X').

voltages. Our BPM results have been exactly matched by MATLAB-based simulation results.

Acknowledgments

The authors would like to acknowledge Indian School of Mines, Dhanbad for financial support for conducting the present research work.

References

1. L. F. Stokes, M. Chodorow, and H. J. Shaw, "All-single-mode fiber resonator," *Opt. Lett.* **7**(6), 288–290 (1982).
2. B. Moslehi et al., "Fiber-optic lattice signal processing," *Proc. IEEE* **72**(7), 909–930 (1984).
3. K. P. Jackson, G. Xiao, and H. J. Shaw, "Coherent optical fibre delay-line processor," *Electron. Lett.* **22**(25), 1335–1337 (1986).
4. N. Takato et al., "Silica-based integrated optic Mach–Zehnder multi/demultiplexer family with channel spacing of 0.01–250 nm," *IEEE J. Sel. Areas Commun.* **8**(6), 1120–1127 (1990).
5. C. Kostrzewa and K. Petermann, "Bandwidth optimization of optical add/drop multiplexers using cascaded couplers and Mach–Zehnder sections," *IEEE Photon. Technol. Lett.* **7**(8), 902–904 (1995).
6. Y. Zhao et al., "Simplified optical millimeter-wave generation configuration by frequency quadrupling using two cascaded Mach–Zehnder modulators," *Opt. Lett.* **34**(21), 3250–3252 (2009).
7. C. C. Wang, "High-frequency narrow-band single-mode fiber-optic transversal filters," *J. Lightw. Technol.* **5**(1), 77–81 (1987).
8. K. Oda et al., "A wide-band guided-wave periodic multi/demultiplexer with a ring resonator for optical FDM transmission systems," *J. Lightw. Technol.* **6**(6), 1016–1023 (1988).
9. G. V. Treyz, "Silicon Mach-Zehnder waveguide interferometers operating at 1.3 μm," *Electro. Lett.* **27**(2), 118–120 (1991).
10. P. A. Besse and H. Melchior, "All-optical switches based on Mach-Zehnder configuration with improved extinction ratios," *IEEE Photo. Technol. Lett.* **9**(1), 55–57 (1997).
11. M. H. Hu et al., "Tunable Mach–Zehnder polarization splitter using height-tapered Y-branches," *IEEE Photo. Technol. Lett.* **9**(6), 773–775 (1997).
12. N. Yoshimoto et al., "High-input-power saturation properties of a polarization-insensitive semiconductor Mach–Zehnder interferometer gate switch for WDM applications," *IEEE Photo. Technol. Lett.* **10**(4), 531–533 (1998).
13. N. S. Lagali et al., "Analysis of generalized Mach-Zehnder interferometers for variable ratio power splitting and optimized switching," *J. Lightwave Technol.* **17**(12), 2542–2550 (1999).
14. R. Schreieck et al., "Ultrafast switching dynamics of Mach–Zehnder interferometer switches," *IEEE Photo. Technol. Lett.* **13**(6), 603–605 (2001).
15. J. J. G.M. vander Tol, H. de Waardt, and Y. Liu, "A Mach–Zehnder-interferometer-based low-loss combiner," *IEEE Photo. Technol. Lett.* **13**(11), 1197–1199 (2001).
16. C. T. Zheng et al., "Investigation on push pull polymer Mach-Zehnder interferometer electro-optic switches using improved 3-D mode propagation analysis method," *Opt. Quant. Electron.* **42**(5), 327–346 (2011).
17. T. Mizuno et al., "Uniform wavelength spacing Mach-Zehnder interferometer using phase-generating couplers," *J. Lightwave Technol.* **24**(8), 3217–3226 (2006).
18. S. Kumar, I. B. Pauria, and A. Singhal, "Optical fiber communication system performance using MZI switching," *Int. J. Soft Comput. Eng.* **2**(3), 98–107 (2012).
19. S. K. Raghuwanshi et al., "Propagation study of Y-branch having inbuilt optical splitters and combiner using beam propagation method, in *Progress in Electromagnetics Research Symp. Proc.*, pp. 720–724 (2012).
20. R. K. Shevgaonkar, "Speakfirst," *L28-Integrated Optics-I* [Video], (2011), http://nptel.iitm.ac.in/courses/117101002/28 (5 November 2012).

Sanjeev Kumar Raghuwanshi is an assistant professor at Electronics Engineering Department of Indian School of Mines, Dhanbad. He is working in the area of optical fiber communication. He received a PhD degree in the field of fiber optics from the Department of Electrical Communication Engineering of I.I.Sc. Bangalore, India, in 2009. He has also authored a book titled *Contemporary Optical Fiber Technology* published by Agrawal Publication, Agra, India, in 2011. He has also contributed one chapter in *Optical Network: Current Issue and Review* published by IGI Global, USA. He has implemented one project on modeling of wavelength-division multiplexing optical components finance by Indian School of Mines, Dhanbad. He has published over 30 research papers in reputed national and international journals and presented about 40 research papers in different national and international conferences, including *IEEE*. He is a member of *IEEE*. Currently, he is guiding five PhD students. He is faculty in charge of electronics engineering, Indian School of Mines, Dhanbad.

Ajay Kumar received a bachelor's degree in electronics and instrumentation engineering from National Institute of Science and Technology, Berhampur, Orissa, India, and a master's degree in electronics and communication engineering from Indian School of Mines, Dhanbad, India. He is pursuing his PhD degree from the Department of Electronics Engineering, Indian School of Mines, Dhanbad, under the guidance of Dr. S. K. Raghuwanshi. He is working in the area of optical fiber communication. He is a graduate member of the Institute of Electrical and Electronics Engineers. He is receiving the MHRD scholarship for his PhD from the Indian School of Mines, Dhanbad.

Santosh Kumar received a bachelor's degree in electronics and communication from the Marathwada Institute of Technology, Aurangabad, Maharashtra. He is pursuing his PhD degree from the Department of Electronics Engineering, Indian School of Mines, Dhanbad under the guidance of Dr. S. K. Raghuwanshi. He is working in the area of optical fiber communication. His research interest is inhomogeneous/non-uniform optical waveguides. He has published papers in reputed journals as well as in conferences, including the IEEE. He is receiving the full scholarship for his PhD research from the Indian School of Mines, Dhanbad. He is a graduate member of the IEEE. He is also a member of SPIE.